THE JOURNAL OF GENE MEDICINE
J Gene Med 2012; **14**: 279–287.
Published online in Wiley Online Library (wileyonlinelibrary.com) **DOI:** 10.1002/jgm.1608

RESEARCH ARTICLE

Effect of vascular endothelial growth factor gene transfer on infarct size, left ventricular function and myocardial perfusion in sheep after 2 months of coronary artery occlusion

Gustavo L. Vera Janavel[1,4]
Andrea De Lorenzi[2]
Claudia Cortés[2]
Fernanda D. Olea[1]
Patricia Cabeza Meckert[3]
Andrés Bercovich[4]
Marcelo Criscuolo[4]
Rubén Laguens[3]
Alberto Crottogini[1]*

[1]*Department of Physiology, Favaloro University, Buenos Aires, Argentina*

[2]*Favaloro University Hospital, Buenos Aires, Argentina*

[3]*Department of Pathology, Favaloro University, Buenos Aires, Argentina*

[4]*Bio Sidus, Buenos Aires, Argentina*

*Correspondence to: A. Crottogini, Department of Physiology, Favaloro University, Solís 453, 1078 Buenos Aires, Argentina.
E-mail: crottogini@favaloro.edu.ar

Received: 14 February 2011
Revised: 30 August 2011
Accepted: 06 September 2011

Abstract

Background In large mammalian models of acute myocardial infarction (AMI), plasmid-mediated vascular endothelial growth factor (pVEGF) gene transfer has been shown to induce angio-arteriogenesis, proliferation of myocyte precursors and adult cardiomyocyte mitosis, reducing infarct size at 15 days after coronary artery occlusion. However, it is unknown whether these effects persist at longer follow-up times, nor how they affect cardiac performance. We thus assessed infarct size, left ventricular (LV) function and perfusion in 2-month-old ovine AMI.

Methods Adult sheep with coronary artery occlusion were randomized to blindly receive ten intramyocardial injections of 3.8 mg of pVEGF or empty plasmid distributed at the infarct border. Three and 60 days later, LV perfusion (single-photon emission computed tomography) and function (stress echocardiography) were assessed. Finally, hemodynamics (LV catheterization), scar size and peri-infarct histology were studied.

Results Infarct size was 30% smaller in pVEGF-treated sheep ($23.6 \pm 1.9\%$ versus $32.7 \pm 2.7\%$ of the LV; $p < 0.02$). Percentage fractional shortening and wall thickening at the infarct border improved after pVEGF, as did myocardial perfusion and LV wall motion under pharmacological stress. Global LV function did not differ between groups, although the force-frequency response was preserved in pVEGF group and lost in placebo animals. These effects were associated with angio-arteriogenesis and proliferation of cardiomyocyte precursors.

Conclusions In sheep with AMI, pVEGF gene transfer affords long-term infarct size reduction, yielding regional LV function and perfusion improvement and reducing remodeling progression. These results suggest the potential usefulness of this approach in the clinical setting.

Keywords angiogenesis; gene therapy; myocardial infarction; remodeling; sheep; VEGF

Introduction

After acute myocardial infarction (AMI), the severity of the left ventricular (LV) remodeling process that leads to heart failure is associated with the extent of the infarct [1,2]. Thus, efforts directed to limit AMI size are of great interest [3,4].

One of the approaches tested in the past few years to attain this goal in large mammalian models of AMI is the transfer of genes coding for diverse growth factors either by intracoronary infusion or intramyocardial injection. In this regard, we have previously reported that plasmid-mediated human vascular endothelial growth factor (VEGF) gene transfer in pigs with chronic myocardial ischemia induces not only angio-arteriogenesis [5], but also entrance in mitosis of adult cardiomyocytes [6] and cardiomyocyte hyperplasia [7]. More recently, we have shown in sheep that intramyocardial injection of 3.8 mg of naked plasmid encoding the VEGF gene 1 h after coronary ligation improves myocardial perfusion and reduces infarct size by 30% 15 days later [8]. The involved mechanisms, assessed at 7 and 10 days after AMI, were a combination of angio-arteriogenesis, reduced peri-infarct fibrosis and decreased myofibroblast proliferation. We also found evidence of cardiomyocyte regeneration, particularly cardiomyoblast proliferation and enhanced mitosis of adult cardiomyocytes, with occasional cytokinesis, 10 days after VEGF gene transfer. Efficient gene transfection of smooth muscle cells and cardiomyocytes yielded a transient VEGF mRNA and protein up-regulation, with a peak expression observed at 3 and 10 days after gene transfer, respectively.

Myocardial infarcts have been shown to expand over time [3,9]. It is therefore important to assess, especially in large infarcts, whether the scar limiting effects of VEGF gene transfer are still present at longer times after AMI. Moreover, in our previous study, regional LV function did not improve significantly, most likely because the short time that elapsed between the expression of the transgene and the moment of evaluation did not allow for functional recovery of hibernating zones. Therefore, in the present study, we also investigated if, at longer follow-up time, plasmid-mediated VEGF gene transfer exerts any effects on global and regional LV function, including the force–frequency response (FFR), whose abnormality is an early indicator of progression to myocardial remodeling and heart failure [10].

Materials and methods

All procedures were carried out in accordance with the Guide for Care and Use of Laboratory Animals, published by the US National Institutes of Health (NIH publication No. 85–23, revised 1996) and approved by the Laboratory Animal Care and Use Committee of the Favaloro University.

Plasmid construct

The naked DNA plasmid, including the human $VEGF_{165}$ coding gene (pVEGF) and the cytomegalovirus promoter/enhancer (Bio Sidus, Buenos Aires, Argentina), is an eukaryotic expression vector of 3930 bp (deposited as pBSVEK3 at *Deutsche Sammlung von Mikroorganismen und Zellkulturen*, accession number DSM14346). The placebo plasmid (3317 bp) is obtained by excision of the human $VEGF_{165}$ coding gene.

Surgical preparation and experimental protocol

Sixteen Corriedale male sheep weighing 24 ± 0.5 kg were operated on. After premedication with intramuscular acepromazine maleate (0.5 mg/kg), anesthesia was induced with intravenous sodium thiopental (20 mg/kg) and maintained with 1.5% halothane in pure oxygen under mechanical ventilation (Neumovent 910; Tecme SA, Córdoba, Argentina). After a sterile thoracotomy at the fourth intercostal space, the left anterior descending artery (LAD) was ligated at its distal third. The second diagonal branch was also ligated at a point in line with the LAD ligature [11]. Anti-arrhythmic drugs were administered intra-operatively as previously described [8].

A total of 32 vials (two for each animal) had been previously coded by the manufacturer such that eight pairs corresponded to pVEGF and eight pairs to placebo. The code was kept blinded for all participants of the study until the end of the data processing. One hour after coronary occlusion, one pair of vials was randomly selected and the injection procedure was started. VEGF-treated sheep ($n = 8$) received 2 ml of a solution containing 1.9 mg/ml of pVEGF and placebo-treated sheep ($n = 8$) received empty plasmid (total dose 3.8 mg). Ten intramyocardial injections (0.2 ml each) were distributed in the peri-infarct normoperfused tissue. The first five injections formed a row 10 mm distant from the border of the ischemic zone, which was easily individualized by the presence of cyanosis and dyskinesia. The remaining injections were made approximately 5 mm distal from the first row. The needle was devised to allow penetration 5 mm into the wall perpendicular to the epicardium. Once the injectate had been pushed, 10 s were allowed to elapse before withdrawing the syringe. Finally, the thoracotomy was repaired and intravenous cephalotin (30 mg/kg) was administered.

Three and 60 days after AMI, LV function and perfusion were assessed. Finally, cardiac catheterization for hemodynamic assessment was performed, animals were killed with an overdose of sodium thiopental followed by a bolus injection of potassium chloride and the heart was excised.

LV function

Bidimensional echocardiography (Sonos 5500; Hewlett Packard, Boston, MA, USA) was performed in conscious, resting conditions and under pharmacological challenge. The stress protocol consisted of increasing doses of intravenous dobutamine under electrocardiographic monitoring until the heart rate increased at least 50% above rest values (or until it had increased above 200 beats/min), as previously described [5]. Figure 1 shows echo images of a protocol sheep at rest. In accordance with standard

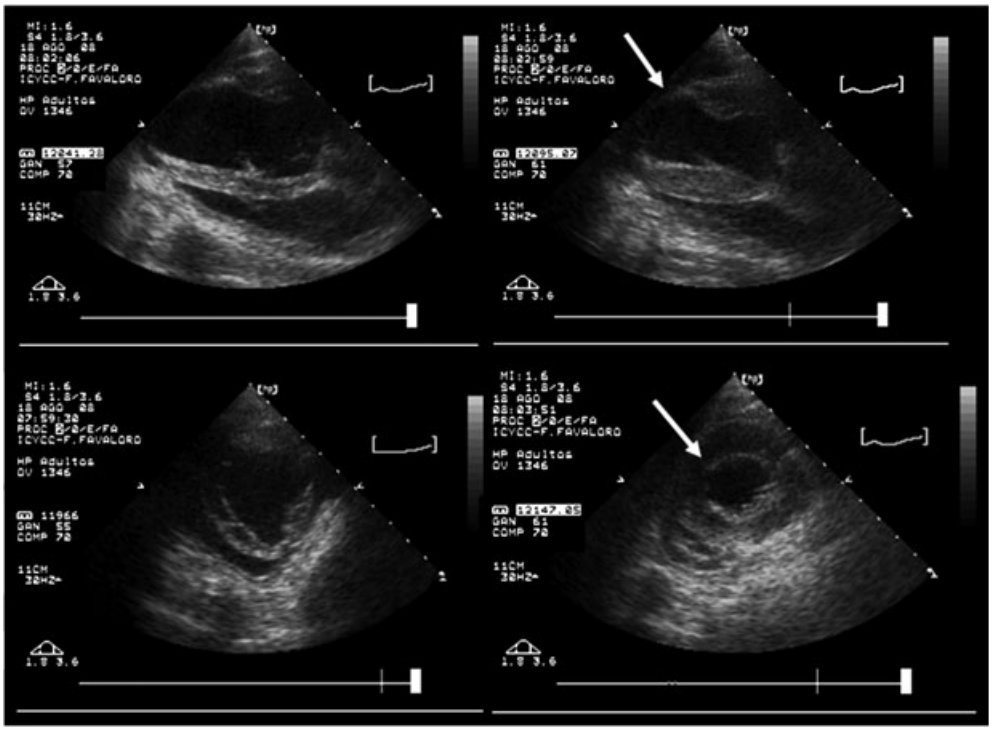

Figure 1. Bidimensional long-axis view (upper panel) and short-axis view (lower panel) of ovine left ventricle at end diastole (left) and end systole (right). A large dyskinetic area is observed in the anterior-apical wall (arrows), especially in the long-axis view.

guidelines [12], percentage LV anterior wall thickening (WTh%), percentage fractional shortening (FS%) and the wall motion score (WMS) of the anterior wall were measured at the infarct border zone. The WMS takes into account the degree of wall dysfunction, assigning 1 point to normokinesia, 2 points to hypokinesia, 3 points to akinesia and 4 points to dyskinesia. Mid-ventricular diameters at end diastole (EDD) and end systole (ESD), as well as LV percentage fractional area change (FAC%), were assessed. LV ejection fraction (EF%) was measured using the Teichholz method.

LV perfusion

LV perfusion at rest and under pharmacological challenge was assessed on 2 consecutive days using single photon emission computed tomography (SPECT) on an ADAC Vertex Dual Detector Camera System (ADAC Vertex, Milpitas, CA, USA). The stress protocol was performed as described above. ^{99m}Tc-sestamibi was injected at conscious state and image acquisition was performed 2 h later. Using the 20 segments model of the LV [13], the summed stress score (SSS) and summed rest score were calculated by two independent observers to obtain the summed difference score (SDS), which quantifies the amount of ischemic myocardium [14].

Hemodynamics and cardiac catheterization

Before sacrifice, LV catheterization was performed with a pressure tip catheter (Millar MikroTip; Millar Instruments Inc., San Diego, CA, USA) under sedation with sodium thiopental. The transducer control unit (TC-510; Millar Instruments) was connected to an amplifier (Gould 2400S; Gould Electronics, Cleveland, OH, USA), a monitor (Sirecust 404–1; Siemens, Berkeley, CA, USA) and a computer with the aid of an A/D expansion card. After calibration, the catheter was introduced into the right carotid artery and then advanced into the LV to acquire the intraventricular pressure signal (frequency: 250 Hz). Heart rate, peak systolic pressure, end diastolic pressure and the peak rates of LV pressure increase and decay (dP/dt_{MAX} and dP/dt_{MIN}, respectively) were calculated using software developed in our laboratory. For each variable, we averaged the values of all beats recorded during a 10-s acquisition time. To obtain the FFR, we fitted the individual values for dP/dt_{MAX} and heart rate to a linear equation [15] and calculated Pearson's coefficient of correlation. The same method was employed to calculate the correlation between dP/dt_{MIN} and heart rate.

Cardiac output (thermodilution) was measured after introducing a Swan–Ganz catheter in the right jugular vein and advancing it to the wedge position. The value for cardiac output (calculated from the average of four measurements) was divided by the body surface area to obtain cardiac index (CI).

Infarct size measurement

After sacrifice, the heart was removed and the LV was opened through an incision parallel to the posterior interventricular sulcus and extended flat before fixation.

DOI: 10.1002/jgm

Digital photographs were obtained for image processing and morphometry with a digital analysis system (Image-Pro Plus 4.1; Media Cybernetics, Silver Spring, MD, USA).

The whole heart was immersed in 10% buffered formaldehyde. After at least 48 h of fixation, 5-mm thick transversal slices were obtained at the level of the infarct border zone and were then embedded in paraffin, sectioned at 4 μm and stained with hematoxilin and eosin or processed for immunohistochemistry (see below). Infarct area was calculated from the average of endocardial and epicardial areas. Infarct size was expressed as a percentage of the total LV area.

Immunohistochemistry

Tissue sections were deparaffinized and brought to phosphate-buffered saline, pH 7.2. After blocking endogenous peroxidase with 3% H_2O_2 in methanol and antigen retrieval pretreatment with citrate buffer in a microwave oven, the slides were incubated for 1 h with specific monoclonal antibodies against Ki67 antigen (Novocastra, Newcastle upon Tyne, UK) for cells into the cell cycle; smooth muscle actin (Biogenex, San Ramon, CA, USA) and von Willebrand factor (Dako, Carpinteria, CA, USA) for blood vessels; sarcomeric actin (Vector, Burlingame, CA, USA), cardiac troponin (Vector) and connexin 43 (Vector) for cardiomyocytes; Sca-1 for cardiac stem cells; and human $VEGF_{165}$ (R&D Systems, Minneapolis, MN, USA) for transgene expression, and post-treated with biotinilated anti-mouse immunoglobulin antiserum (Multilink; Biogenex), followed by peroxidase-labeled avidin, revealed with AEC as chromogen and counterstained with hematoxylin. For all antibodies, the dilution used was 1:50. After immunohistochemistry, the surviving myocardium, the infarct and the adjacent border were examined under light microscopy and Nomarski optics or fluorescence microscopy (Zeiss Axiophot; Carl Zeiss, Oberkochen, Germany) equipped with a digital camera (Zeiss AxioCam MRc5). Vessels with smooth muscle actin media layer in the range 8–50 μm in diameter were considered arterioles and counted. Capillaries were counted as well, after identification as vessels positive for von Willebrand immunostain and smaller than 8 μm. Arteriole and capillary numerical densities were calculated for each heart as the number of arterioles or capillaries per mm^2 of total scanned area. Arteriolar length density (*aLd*) was calculated according to the equation:

$$aLd = 1/A \sum_{i=1}^{n} R_i = (R_1 + R_2 + R_3 + \ldots R_n)/A$$

For n vessels encountered in an area A, *aLd* [expressed in mm per unit volume of myocardium (mm/mm^3)] is equal to the sum of the ratio R of the long to the short axis of each vessel [16].

Statistical analysis

The FFR was analyzed with Pearson's R coefficient for linear regression. Fisher's exact test was used to analyze the association between the presence of small cardiomyocytes (see below) and treatment in each group. LV perfusion was analyzed with repeated measures analysis of variance (ANOVA) with the Greenhouse and Geisser correction of degrees of freedom. Lack of normality was corrected with rank transformation. Echocardiography-assessed LV function data were analyzed using Student's t-test for paired data because the uneven number of subjects in each group prevented us from applying ANOVA. Arteriole and capillary numerical and length densities, infarct size, LV hemodynamics and CI were compared using an unpaired Student's t-test. Dicotomic variables are reported as percentages and other results as the mean ± SEM. $p < 0.05$ was considered statistically significant.

Results

Animal loss

Two animals from the placebo group developed refractory ventricular fibrillation during the final perfusion study. Thus, results of LV perfusion, LV function (both regional and global) and hemodynamics (but not of morphometry and histology) for the placebo group are based on data obtained from six animals. Results of LV perfusion for the VEGF group are based on the data obtained from six sheep as a result of poor nuclear scan image quality in two animals. All the remaining results for this group are based data obtained from eight subjects.

Morphometry and histology

Given the terminal nature of ovine coronary circulation, the infarct border was sharply demarcated and the infarcted zone was readily visible. Infarct size was significantly smaller in the VEGF-treated group (placebo: 32.7 ± 2.7%, VEGF: 23.6 ± 1.9%; $p < 0.02$).

With regard to histology, the total scanned area for each heart was 4.3 ± 0.2 mm^2 in the placebo group and 4.4 ± 0.3 mm^2 in the VEGF group (p = not significant). Capillary numerical density was significantly higher in the VEGF-treated group (2120.8 ± 183.6 versus 1532 ± 131.1 capillaries/mm^2; $p < 0.04$). Profuse arteriolar proliferation was observed in VEGF-treated sheep (Figure 2), as indicated by an almost three-fold higher arteriolar numerical density (78.3 ± 12 versus 27.6 ± 0.6 arterioles/mm^2; $p < 0.02$) and arteriolar length density (142.3 ± 18.5 versus 53.7 ± 3.7 mm/mm^3; $p < 0.03$) compared to placebo animals.

Cycling cardiomyocytes and/or mitoses were consistently absent in both groups. We observed clusters of small cells (approximately 4–10 μm in diameter) in the vicinity of the infarct border only in tissue sections of VEGF-treated group (placebo: 0%, VEGF: 75%; $p < 0.01$). These cells stained positive for sarcomeric actin, cardiac troponin and connnexin 43 and negative for Sca-1 (Figure 3).

Human $VEGF_{165}$ immune reactions were consistently negative.

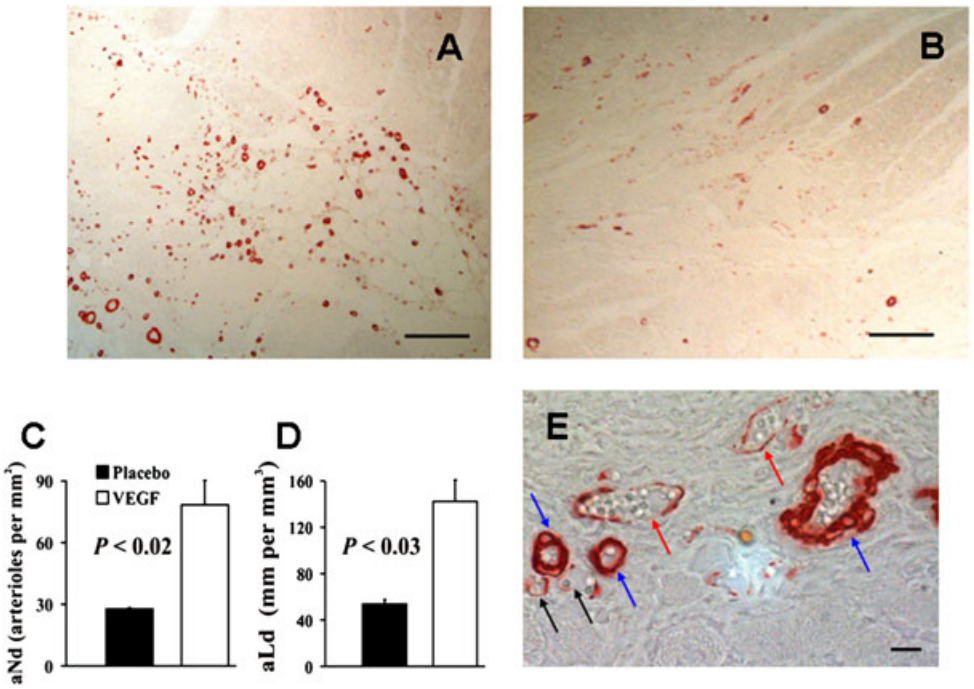

Figure 2. Arteriolar proliferation. (A, B) Tissue sections of the infarct border zone in a VEGF-treated sheep and a placebo-treated sheep, respectively. An intense VEGF-induced arteriogenesis is seen in the former. Scale bars = 200 μm. (C) Arteriolar numerical density (*Nd*) and (D) arteriolar length (*aLd*) at 60 days after acute coronary artery ligation followed by injection of a plasmid coding VEGF or empty plasmid (placebo). (E) A tissue section of the infarct border in a VEGF-treated sheep at high magnification. Microvessls are functional, as indicated by the presence of red blood cells in capillaries (black arrows), venules (red arrows) and arterioles (blue arrows). Nomarski optics. Scale bar = 10 μm.

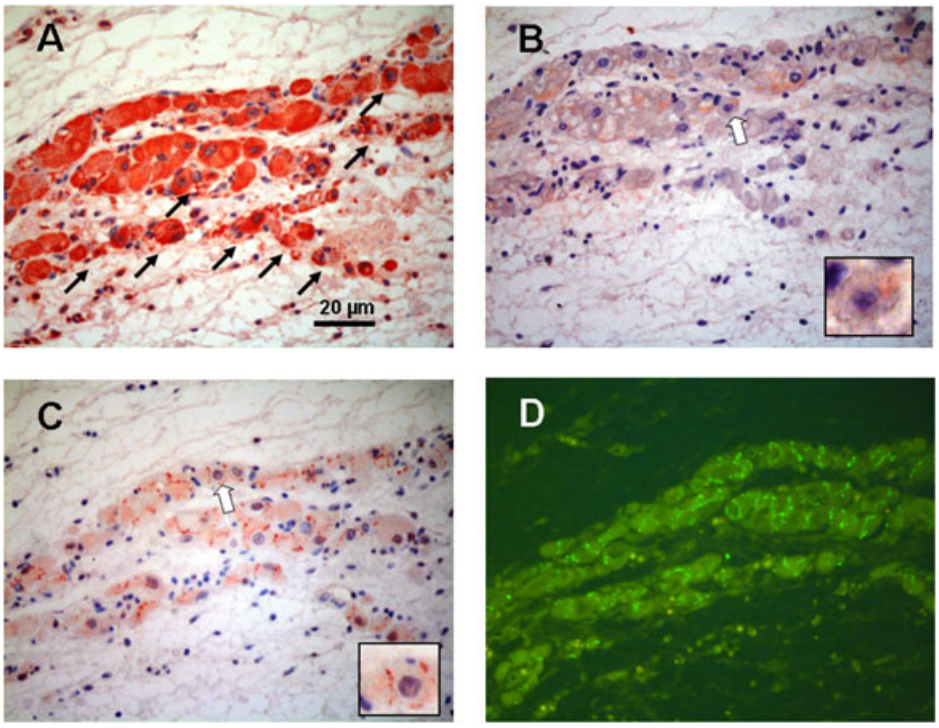

Figure 3. Immunohistochemistry of cardiomyocyte markers. (A) A cluster of small rounded cells (arrows) displaying sarcomeric actin in their cytoplasm. These cells also contain cardiac troponin (B) and connexin 43 (C). (D) An immnofluorescence image of connexin 43 in more detail. The insets in (B) and (C) show, at greater magnification, the cells indicated with white arrows.

LV perfusion

Basal, preocclusion LV myocardial perfusion was normal in all animals. In placebo sheep, neither the SSS, nor the SDS changed between 3 and 60 days after AMI (SSS: 26.3 ± 6.1 versus 24.7 ± 4.4; SDS: 4.7 ± 3.2 versus 3.3 ± 2.1 after AMI; p = not significant), revealing steady peri-infarct ischemia. By contrast, in VEGF sheep, peri-infarct myocardial

DOI: 10.1002/jgm

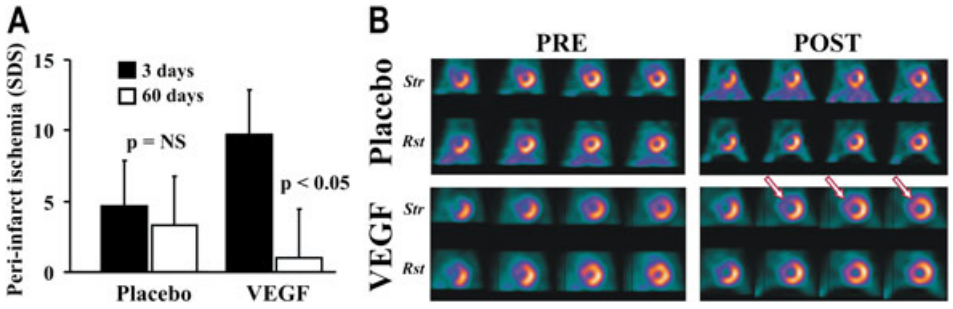

Figure 4. Myocardial perfusion. (A) Peri-infarct ischemia, as assessed by the SDS calculated from single photon emission computed tomography scan, decreased significantly over time in the group injected with the plasmid coding VEGF but not in the group injected with empty plasmid (placebo). (B) Tomographic left ventricular short axis slices at rest (Rst) and under pharmacological stress with dobutamine (Str) in a placebo- and a VEGF-treated sheep show peri-infarct ischemia at 3 days after coronary artery ligation (PRE) in both animals. At 60 days (POST), the placebo sheep exhibits worse perfusion at rest and stress, whereas the VEGF-treated sheep shows a similar image at rest but a marked decrease of the perfusion defect under stress (arrows).

perfusion improved, as indicated by a decrease in SDS from 9.7 ± 3.5 at 3 days to 1 ± 0.5 at 2 months after AMI ($p < 0.05$) (Figure 4), which was accompanied by a decrease in SSS from 37.5 ± 2.4 to 31.2 ± 1.7 ($p < 0.05$).

LV function

Table 1 shows the echocardiographic results for regional and global LV function. At the peri-infarct surviving myocardium of the LV anterior wall, WTh% improved over time in the VEGF-treated group but not in the placebo group. Similarly, peri-infarct FS% showed a significant increase in VEGF-treated sheep but not in placebo animals.

As regarding LV dimensions, mid-ventricular EDD did not change significantly over time in VEGF-treated or placebo-treated sheep. ESD, on the other hand, showed a slight, although significant increase in the VEGF-treated group. Although proportionally equal, the change in ESD in the placebo group did not attain statistical significance. Mid-ventricular FAC% did not vary over time either in VEGF- or placebo-treated sheep, nor did global LV EF%.

The WMS at the infarct border zone early after AMI revealed similarly impaired wall kinetics in both groups (placebo: 2.8 ± 0.1 at rest and 2.8 ± 0.1 during stress, p = not significant; VEGF: 2.7 ± 0.2 at rest and 2.6 ± 0.2 during stress, p = not significant). However, 2 months later, VEGF-treated sheep exhibited myocardial viability at the infarct border (2.8 ± 0.2 at rest and 2.1 ± 0.2 during stress; $p < 0.05$), as opposed to placebo sheep, in which that region remained akinetic (3 ± 0 at rest and 3 ± 0 during stress; p = not significant).

Hemodynamics and FFR

None of the variables obtained from right and left ventricular catheterization differed between groups (Table 2). By contrast, FFR was preserved in the VEGF-treated group ($R = 0.94$, $p < 0.001$) but was markedly deteriorated in the placebo group ($R = 0.3$, p = not significant) (Figure 5A). Furthermore, the correlation between the lusitropic index (dP/dt_{MIN}) and heart rate remained normal in VEGF-treated sheep ($R = -0.87$, $p < 0.005$) but was blunted in placebo animals ($R = -0.45$, p = not significant) (Figure 5B). Because LV end-diastolic and peak pressures were similar between groups (p = not significant) (Table 2), LV loading conditions did not bias dP/dt rates of placebo and VEGF-treated groups.

Discussion

When studying infarct size limitation in large mammals, pigs or sheep are usually used. We chose sheep because, unlike pigs, whose cardiomyocytes have up to 32 nuclei,

Table 1. Regional and global left ventricular function at 3 and 60 days after myocardial infarction

	Placebo			VEGF		
	3 days	60 days	*p*	3 days	60 days	*p*
WTh (%)	9.6 ± 6.2	11.4 ± 7.4	NS	9.9 ± 3	24.8 ± 8.1	< 0.05
FS (%)	22 ± 2.3	25.5 ± 4.4	NS	19.2 ± 2.6	31.6 ± 3.6	< 0.01
EDD (mm)	33.7 ± 2.5	37.9 ± 1.4	NS	35.7 ± 1.1	38 ± 1.8	NS
ESD (mm)	22.8 ± 0.8	25.9 ± 2	NS	24 ± 1	27.3 ± 0.6	< 0.05
FAC (%)	41.2 ± 3.4	48.5 ± 3	NS	45.3 ± 3.6	50.1 ± 1.5	NS
EF (%)	45.6 ± 1.9	42.9 ± 4.5	NS	42.3 ± 3.0	41.5 ± 3.4	NS

WTh, peri-infarct percentage wall thickening; FS, peri-infarct percentage circumferential fiber shortening; EDD, mid-ventricle end diastolic diameter; ESD, mid-ventricle end systolic diameter; FAC, mid-ventricle percentage fractional area change; EF, ejection fraction; NS, not significant.

DOI: 10.1002/jgm

Table 2. Hemodynamics

	Placebo	VEGF	*p*
CI (l/min/m^2)	4.3 ± 0.2	4.1 ± 0.3	NS
HR (beats/min)	137.3 ± 4.8	129.5 ± 8.4	NS
PSP (mmHg)	123.1 ± 1.8	119.4 ± 6.3	NS
EDP (mmHg)	6.2 ± 0.7	8.3 ± 0.8	NS
dP/dt_{MAX} (mmHg/sec)	2515.2 ± 169.4	2171.5 ± 348.7	NS
dP/dt_{MIN} (mmHg/sec)	−2891.6 ± 131.5	−2808.4 ± 292.5	NS

CI, cardiac index; HR, heart rate; PSP, peak systolic pressure; EDP, end-diastolic pressure; dP/dt_{MAX}, peak rate of left ventricular pressure increase; dP/dt_{MIN}, peak rate of left ventricular pressure decay; NS, not significant.

ovine cardiomyocytes have only one to four nuclei [17], thus being more similar to the humans. In addition, pigs are more prone to develop irreversible ventricular fibrillation than sheep, thus leading to higher mortality.

We have previously shown in adult sheep that, after 15 days of permanent coronary artery ligation, a plasmid encoding human $VEGF_{165}$, injected intramyocardially at the time of occlusion, reduces infarct size by a combination of angio-arteriogenesis, cardiomyogenesis and anti-fibrogenesis [8].

Given that the infarcts progressively expand into normoperfused zones over time [3,9], we now tested whether the scar size limiting effect was still present in the long term. Our results show that, 2 months after coronary occlusion, the infarcts of pVEGF-transfected sheep are approximately 30% smaller than those of sheep receiving placebo. In addition, VEGF improved regional LV function significantly (which is an effect that was not attained in our previous study) and preserved the FFR, an early pathophysiologic predictor of ventricular remodeling and failure [10]. These effects were associated with a remarkable angio-arteriogenic response resulting in almost three-fold higher arteriolar numerical and length densities in pVEGF-treated animals. The higher capillary and arteriolar densities found in VEGF-treated sheep indicate that the induced vasculature or, at least, most of it, persisted 60 days after the stimulus of a single gene transfer. Although red blood cells could be seen in most capillaries and arterioles (Figure 2E), we cannot state with certainty that all the neoformed microvessels were functional. However, the SPECT data suggest that a significant percentage of them were, on account of the fact that the overall angio-arteriogenic response resulted in improved perfusion to the peri-infarct myocardium. Because coronary angiography was not performed, we cannot rule out the possibility that large epicardial collaterals developed. However, this has not been the case in our previous studies on pigs with chronic myocardial ischemia, in which coronary angiography was performed [5].

It should be noted that the dose used in the present study, as well as in our previous studies, is eight-fold higher than that used in the Euroinject trial [18] and two-fold higher than that used in the NORTHERN trial [19], comprising the two phase II clinical trials reported so far. The dose is an important issue when working with plasmids on account of the low transfection efficiency of naked DNA. Viral vectors, in contrast, are more efficient, although they entail the risk of immune reaction should the treatment be repeated. For adeno-associated viruses, on the other hand, aberrant angiogenesis and fibrosis as a result of long-term unregulated protein expression has been reported [20].

Concerning gene expression, we previously showed that, in this animal model, plasmid-VEGF gene expression is transient, with mRNA peaking at 3 days post-transfection and becoming indetectable at later time points. Human VEGF protein, on the other hand, is positive in the transfected myocardium at 7 days and remains detectable until 35 days post-transfection [8]. In the light of those results, the absence of the human $VEGF_{165}$ protein in the myocardium of the present sheep, killed at 60 days post-transfection, was to be expected.

In our previous work, other VEGF-induced mechanisms, particularly adult cardiomyocyte mitosis and myoblast proliferation, were involved in infarct size reduction. These phenomena were found to occur early after treatment, with cycling adult myocytes and myoblasts being

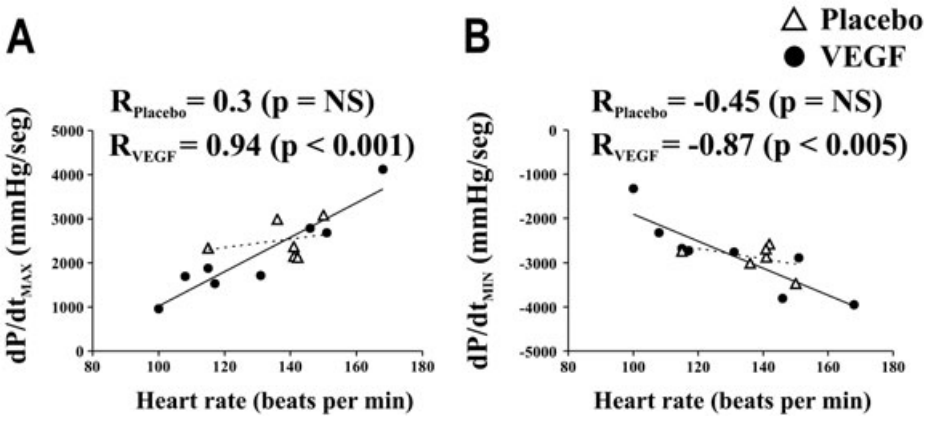

Figure 5. FFR. (A) Pearson's correlation (*R*) between the peak rate of left ventricular pressure increase (dP/dt_{MAX}) and heart rate in sheep 60 days after coronary artery ligation followed by injection of a plasmid encoding VEGF or empty plasmid (placebo). Unlike placebo animals, VEGF-treated sheep show preservation of the normal linearity of the FFR. (B) Correlation between the peak rate of left ventricular pressure decay (dP/dt_{MIN}) and heart rate, showing preserved normal linearity only in VEGF-treated sheep.

DOI: 10.1002/jgm

profusely present at 10 but not at 15 days after gene transfer. In the present study, however, there was no evidence of adult cardiomyocyte proliferation. A comment should be made on the clusters of small cells that VEGF-treated hearts showed in the periphery of the infarcted zone. Given their positive reaction for cardiomyocite markers, it may be assumed that these cells could represent those described and referred to as 'small developing cardiomyocytes' for the human heart [21–23]. Their negative reaction to the Sca-1 antibody is consistent with the fact that, at this stage of lineage commitment, these cells no longer express their surface stem cell antigens. Whether or not these cells remain small or eventually reach the size of adult cardiomyocytes over the long-term cannot be established from our present results.

Because remodeling progression depends on the extension of the necrotic area [1,3], the present protocol was designed to induce large myocardial infarcts (approximately 30% of the LV area) and to study a variable that would permit early recognition of myocardial remodeling, namely the FFR.

The capability of raising myocardial contractility in response to increased heart rate (also known as the Bowditch effect) is a key mechanism for normal cardiac adaptation to acute augmentations in work load [24,25]. A negative, blunted or absent FFR is recognized as a signature abnormality among failing hearts from humans and animal models [15,26–28]. Moreover, it has been demonstrated that an abnormal FFR is a reliable pathophysiologic sign of the cardiomyopathic state, even when contractility at slow stimulation frequencies is not yet reduced [10]. We found that VEGF-treated sheep had a normal FFR, as indicated by a high and significant correlation between dP/dt_{MAX} and heart rate, whereas it was markedly deteriorated in placebo animals. Additionally, our results showed preservation of the relationship between dP/dt_{MIN} and heart rate, suggesting a beneficial effect of VEGF on myocardial lusitropic state.

Numerous studies have investigated the possible mechanisms underlying abnormal FFR in failing hearts, and the vast majority of them agree that either myocyte Ca^{2+} cycle defects [10] or frequency-dependent myofilament Ca^{2+} desensitization [29] are implicated.

Our work was not designed to study the underlying reasons for FFR preservation, although it might have been related to better perfusion, lesser jeopardized myocardium and higher contractile mass. Moreover, VEGF could have acted also on distant territories, as supported by previous results in pigs showing that VEGF acts in remote zones, inducing arteriolar growth [5] and increasing the mitotic index of adult cardiomyocytes in non-injected, non-ischemic territories [6]. Nevertheless, these reasonings are speculative, and future work addressing this subject is needed.

With regard to regional myocardial function, in our previous work, its tendency to improve in the VEGF group (as assessed by gated SPECT) failed to achieve significance. This was attributed to the persistence of regional hibernation resulting from the short time that had elapsed between the establishment of the VEGF-induced neovasculature and regional function assessment. This reasoning is supported by our present results, showing that, at longer follow-up, not only regional myocardial perfusion, but also wall kinetics improve significantly. Furthermore, the lower echocardiographic stress wall motion score at 2 months post-AMI reveals functional recruitment of previously akinetic zones in VEGF-treated sheep, contrasting with the placebo group, whose invariably high wall motion score under stress indicates persistent akinesia at the AMI border zone. However, these regional function improvements were not accompanied by enhanced global LV performance, as indicated by an unchanged EF%.

In conclusion, plasmid-mediated human $VEGF_{165}$ gene transfer in adult sheep with 2 months of permanent coronary artery occlusion reduces infarct size, improves regional LV function and perfusion, and reduces remodeling progression. These results suggest that transfecting the $VEGF_{165}$ gene remains a possible alternative for the treatment of diseases characterized by myocardial cell loss.

Acknowledgements

We thank the technicians: Julio Martínez, Fabián Gauna and Marcela Álvarez; veterinarians: María Inés Besansón, Pedro Iguain and Marta Tealdo; and animal house personnel: Juan Ocampo, Osvaldo Sosa and Juan Mansilla. This work was supported by grant BID 1728/OC-AR PID 268 from the National Agency for Scientific and Technological Promotion (ANPCyT) of Argentina. Dr A. Crottogini is an established Investigator of National Council for Scientific and Technical Investigations of Argentina (CONICET).

Conflicts of interest statement

GVJ, AB and MC are scientists of Bio Sidus SA, the biotechnological company that developed the plasmid used in the present study. No financial support was provided by the company.

References

1. Sutton MG, Sharpe N. Left ventricular remodeling after myocardial infarction: pathophysiology and therapy. *Circulation* 2000; **101**: 2981–2988.
2. Yankey GK, Li T, Kilic A, *et al*. Regional remodeling strain and its association with myocardial apoptosis after myocardial infarction in an ovine model. *J Thorac Cardiovasc Surg* 2008; **135**: 991–998.
3. Jackson BM, Gorman JH, Moainie SL, *et al*. Extension of borderzone myocardium in postinfarction dilated cardiomyopathy. *J Am Coll Cardiol* 2002; **40**: 1160–1171.
4. Laguens RP, Crottogini AJ. Cardiac regeneration: the gene therapy approach. *Expert Opin Biol Ther* 2009; **9**: 411–425.

5. Crottogini A, Cabeza Meckert P, Vera Janavel G, *et al*. Arteriogenesis induced by intramyocardial vascular endothelial growth factor 165 gene transfer in chronically ischemic pigs. *Hum Gene Ther* 2003; **14**: 1307–1318.
6. Laguens R, Cabeza Meckert P, Vera Janavel G, *et al*. Entrance in mitosis of adult cardiomyocytes in ischemic pig hearts after plasmid-mediated rhVEGF165 gene transfer. *Gene Ther* 2002; **9**: 1676–1681.
7. Laguens R, Cabeza Meckert P, Vera Janavel G, *et al*. Cardiomyocyte hyperplasia after plasmid-mediated vascular endothelial growth factor gene transfer in pigs with chronic myocardial ischemia. *J Gene Med* 2004; **6**: 222–227.
8. Vera Janavel G, Crottogini A, Cabeza Meckert P, *et al*. Plasmid-mediated VEGF gene transfer induces cardiomyogenesis and reduces myocardial infarct size in sheep. *Gene Ther* 2006; **13**: 1133–1142.
9. Erlebacher JA, Weiss JL, Weisfeldt ML, Bulkley BH. Early dilation of the infarcted segment in acute transmural myocardial infarction: role of infarct expansion in acute left ventricular enlargement. *J Am Coll Cardiol* 1984; **4**: 201–208.
10. Rossman EI, Petre RE, Chaudhary KW, *et al*. Abnormal frequency-dependent responses represent the pathophysiologic signature of contractile failure in human myocardium. *J Mol Cell Cardiol* 2004; **36**: 33–42.
11. Markovitz LJ, Savage EB, Ratcliffe MB, *et al*. Large animal model of left ventricular aneurysm. *Ann Thorac Surg* 1989; **48**: 838–845.
12. Schiller NB, Shah PM, Crawford M, *et al*. Recommendations for quantitation of the left ventricle by two-dimensional echocardiography. American Society of Echocardiography Committee on Standards, Subcommittee on Quantitation of Two-Dimensional Echocardiograms. *J Am Soc Echocardiogr* 1989; **2**: 358–367.
13. Hachamovitch R, Berman DS, Kiat H, *et al*. Exercise myocardial perfusion SPECT in patients without known coronary artery disease: incremental prognostic value and use in risk stratification. *Circulation* 1996; **93**: 905–914.
14. Hansen CL, Goldstein RA, Berman DS, *et al*. Quality Assurance Committee of the American Society of Nuclear Cardiology. Myocardial perfusion and function single photon emission computed tomography. *J Nucl Cardiol* 2006; **13**: E97–E120.
15. Ryu KH, Tanaka N, Dalton N, *et al*. Force-frequency relations in the failing rabbit heart and responses to adrenergic stimulation. *J Card Fail* 1997; **3**: 27–39.
16. Adair TH, Wells ML, Hang J, Montani JP. A stereological method for estimating length density of the arterial vascular system. *Am J Physiol* 1994; **266**: H1434–H1438.
17. Adler CP, Friedburg H, Herget GW, Neuburger M, Schwalb H. Variability of cardiomyocyte DNA content, ploidy level and nuclear number in mammalian hearts. *Virchows Arch* 1996; **429**: 159–164.
18. Kastrup J, Jørgensen E, Rück A, *et al*. Direct intramyocardial plasmid vascular endothelial growth factor-A165 gene therapy in patients with stable severe angina pectoris A randomized double-blind placebo-controlled study: the Euroinject One trial. *J Am Coll Cardiol* 2005; **45**: 982–988.
19. Stewart DJ, Kutryk MJ, Fitchett D, *et al*. VEGF gene therapy fails to improve perfusion of ischemic myocardium in patients with advanced coronary disease: results of the NORTHERN trial. *Mol Ther* 2009; **17**: 1109–1115.
20. Karvinen H, Pasanen E, Rissanen TT, *et al*. Long-term VEGF-A expression promotes aberrant angiogenesis and fibrosis in skeletal muscle. *Gene Ther* 2011; May 12; **18**: 1166–1172.
21. Beltrami AP, Barlucchi L, Torella D, *et al*. Adult cardiac stem cells are multipotent and support myocardial regeneration. *Cell* 2003; **114**: 763–776.
22. Urbanek K, Torella D, Sheikh F, *et al*. Myocardial regeneration by activation of multipotent cardiac stem cells in ischemic heart failure. *Proc Natl Acad Sci USA* 2005; **102**: 8692–8697.
23. Hosoda T, Kajstura J, Leri A, Anversa P. Mechanisms of myocardial regeneration. *Circ J* 2010; **74**: 13–17.
24. Hasenfuss G, Holubarsch C, Hermann HP, Astheimer K, Pieske B, Just H. Influence of the force-frequency relationship on haemodynamics and left ventricular function in patients with non-failing hearts and in patients with dilated cardiomyopathy. *Eur Heart J* 1994; **15**: 164–170.
25. Holubarsch C, Ruf T, Goldstein DJ, *et al*. Existence of the Frank-Starling mechanism in the failing human heart. Investigations on the organ, tissue, and sarcomere levels. *Circulation* 1996; **94**: 683–689.
26. Mulieri LA, Hasenfuss G, Leavitt B, Allen PD, Alpert NR. Altered myocardial force-frequency relation in human heart failure. *Circulation* 1992; **85**: 1743–1750.
27. Pieske B, Hasenfuss G, Holubarsch C, Schwinger R, Böhm M, Just H. Alterations of the force-frequency relationship in the failing human heart depend on the underlying cardiac disease. *Basic Res Cardiol* 1992; **87**: 213–221.
28. Li K, Rouleau JL. Tension-frequency relationships in normal and cardiomyopathic dog and hamster myocardium. *J Mol Cell Cardiol* 1995; **27**: 1251–1261.
29. Lamberts RR, Hamdani N, Soekhoe TW, *et al*. Frequency-dependent myofilament Ca^{2+} desensitization in failing rat myocardium. *J Physiol* 2007; **582**: 695–709.